RESEARCH ARTICLE

NUTRIENT METABOLISM

Zonated leucine sensing by Sestrin-mTORC1 in the liver controls the response to dietary leucine

Andrew L. Cangelosi[1,2,3]*, Anna M. Puszynska[1,2], Justin M. Roberts[1,2,3], Andrea Armani[1,2,4,5], Thao P. Nguyen[1,2,3], Jessica B. Spinelli[1,2], Tenzin Kunchok[1], Brianna Wang[1], Sze Ham Chan[1]†, Caroline A. Lewis[1], William C. Comb[1,2]‡, George W. Bell[1], Aharon Helman[6], David M. Sabatini[3]§

The mechanistic target of rapamycin complex 1 (mTORC1) kinase controls growth in response to nutrients, including the amino acid leucine. In cultured cells, mTORC1 senses leucine through the leucine-binding Sestrin proteins, but the physiological functions and distribution of Sestrin-mediated leucine sensing in mammals are unknown. We find that mice lacking Sestrin1 and Sestrin2 cannot inhibit mTORC1 upon dietary leucine deprivation and suffer a rapid loss of white adipose tissue (WAT) and muscle. The WAT loss is driven by aberrant mTORC1 activity and fibroblast growth factor 21 (FGF21) production in the liver. Sestrin expression in the liver lobule is zonated, accounting for zone-specific regulation of mTORC1 activity and FGF21 induction by leucine. These results establish the mammalian Sestrins as physiological leucine sensors and reveal a spatial organization to nutrient sensing by the mTORC1 pathway.

L eucine is an essential amino acid needed to synthesize proteins and metabolites such as branched chain fatty acids (1–3). In addition, it has been recognized for decades that leucine has distinctive physiological effects, including promoting skeletal muscle growth (4–8), insulin secretion (9–11), and immune function (12–14) and modulating health span and life span in mice (15–17). Moreover, plasma leucine concentrations are also implicated in certain pathological states, such as metabolic syndrome (18–20).

A key effector of leucine is thought to be the mechanistic target of rapamycin complex 1 (mTORC1) protein kinase, a master regulator of growth and metabolism. Diverse nutrients, growth factors, and stresses regulate mTORC1 (4, 21–23), and understanding how it detects so many inputs has been of longstanding interest. A model has started to emerge of the nutrient-sensing mechanisms upstream of mTORC1 in which nutrient-derived signals converge on the heterodimeric

Rag guanosine triphosphatases (GTPases) and their many regulators, including the GATOR1, GATOR2, and Ragulator complexes. The Rag heterodimer binds mTORC1 in a nutrient-sensitive manner to control its localization to the lysosomal surface, where it can interact with its kinase activator, the Rheb GTPase (4, 21–23).

How the mTORC1 pathway senses leucine has been highly debated (24–31). Several years ago, we showed that in cultured cells the leucine-binding proteins Sestrin1 and Sestrin2 serve as leucine sensors for the pathway (32, 33). Growing evidence implicates the Sestrins in various facets of organismal function (34–39). However, whether the mammalian Sestrins have a leucine-sensing role in vivo— and, if so, in which tissues they act and the physiology they control as leucine sensors— is unknown.

Results

Sestrin1 and Sestrin2 are physiological leucine sensors for mTORC1

To study leucine sensing by mTORC1 in vivo and minimize confounding effects of other nutrient alterations, we tested the response of mice to changes in dietary leucine content. We first fasted and refed mice with food containing 100, 10, or 0% of the leucine content of standard chow (Fig. 1A). Feeding of these diets caused stepwise reductions in plasma leucine concentrations (Fig. 1B) and in the phosphorylation of the mTORC1 substrates S6K1 (S6 kinase 1) and 4EBP1 (eukaryotic translation initiation factor 4E–binding protein 1) in the liver (Fig. 1C), showing that, in our experimental system, dietary leucine controls mTORC1 activity in vivo.

In cultured cells, Sestrin1 and Sestrin2 inhibit mTORC1 signaling by interacting with and suppressing—in a leucine-sensitive manner— the GATOR2 complex, a positive component of the mTORC1 pathway (32). To determine whether the same interaction occurs in vivo, we immunoprecipitated, from the liver of mice, GATOR2 using an antibody to its WDR24 component. Consistent with leucine disrupting the Sestrin1/2-GATOR2 interaction, GATOR2 coimmunoprecipitated greater amounts of Sestrin1 and Sestrin2 in mice refed the leucine-free than in those fed the control diet (Fig. 1D). Notably, the addition of leucine, but not arginine, to the immunopurified complexes disrupted the Sestrin1/2-GATOR2 interaction (Fig. 1D). Thus, as in cultured cells, leucine regulates the binding of Sestrin1 and Sestrin2 to GATOR2 in vivo in mouse tissues.

To determine whether the regulation of mTORC1 by dietary leucine requires Sestrin1 and Sestrin2, we generated mice lacking both proteins [double-knockout (DKO) mice] and fasted and refed them with the control or leucine-free diet. Whereas mTORC1 activity in the liver was low in wild-type (WT) mice refed with the leucine-free diet, in DKO mice, mTORC1 activity was high, irrespective of the leucine content of the diet in both males (Fig. 1E) and females (fig. S1A). Sestrin expression did not affect food consumption (fig. S1B). Loss of either Sestrin1 or Sestrin2 alone had no impact on the sensitivity of mTORC1 to leucine deprivation (fig. S1, C and D), consistent with Sestrin1 and Sestrin2 having redundant functions in cultured cells (32). As it does in the liver, leucine regulates mTORC1 activity in white adipose tissue (WAT) in a Sestrin-dependent manner in males (Fig. 1F) and females (fig. S1E).

mTORC1 signaling remained sensitive to fasting in the liver and WAT of DKO mice (fig. S2, A and B) and to starvation of all amino acids (but not to starvation of only leucine) in primary hepatocytes and WAT explants obtained from DKO mice (fig. S2, C and D). Thus, loss of the Sestrins affects the response of mTORC1 specifically to leucine deprivation.

The Sestrins have been proposed to impinge on the mTORC1 pathway through regulation of adenosine monophosphate–activated protein kinase (AMPK) (36). However, in our model system, liver-specific deletion of both AMPK catalytic subunits (AMPKα1 and AMPKα2) did not affect the activation of hepatic mTORC1 by dietary leucine, despite eliminating AMPK activity, as indicated by the absence of phosphorylation of acetyl–coenzyme A carboxylase (ACC), a canonical AMPK substrate (fig. S2E).

On the basis of the structure of the leucine-binding pocket of Sestrin2, we previously identified a point mutation [Trp[444]→Leu (W444L)] that reduces, but does not abolish, the affinity
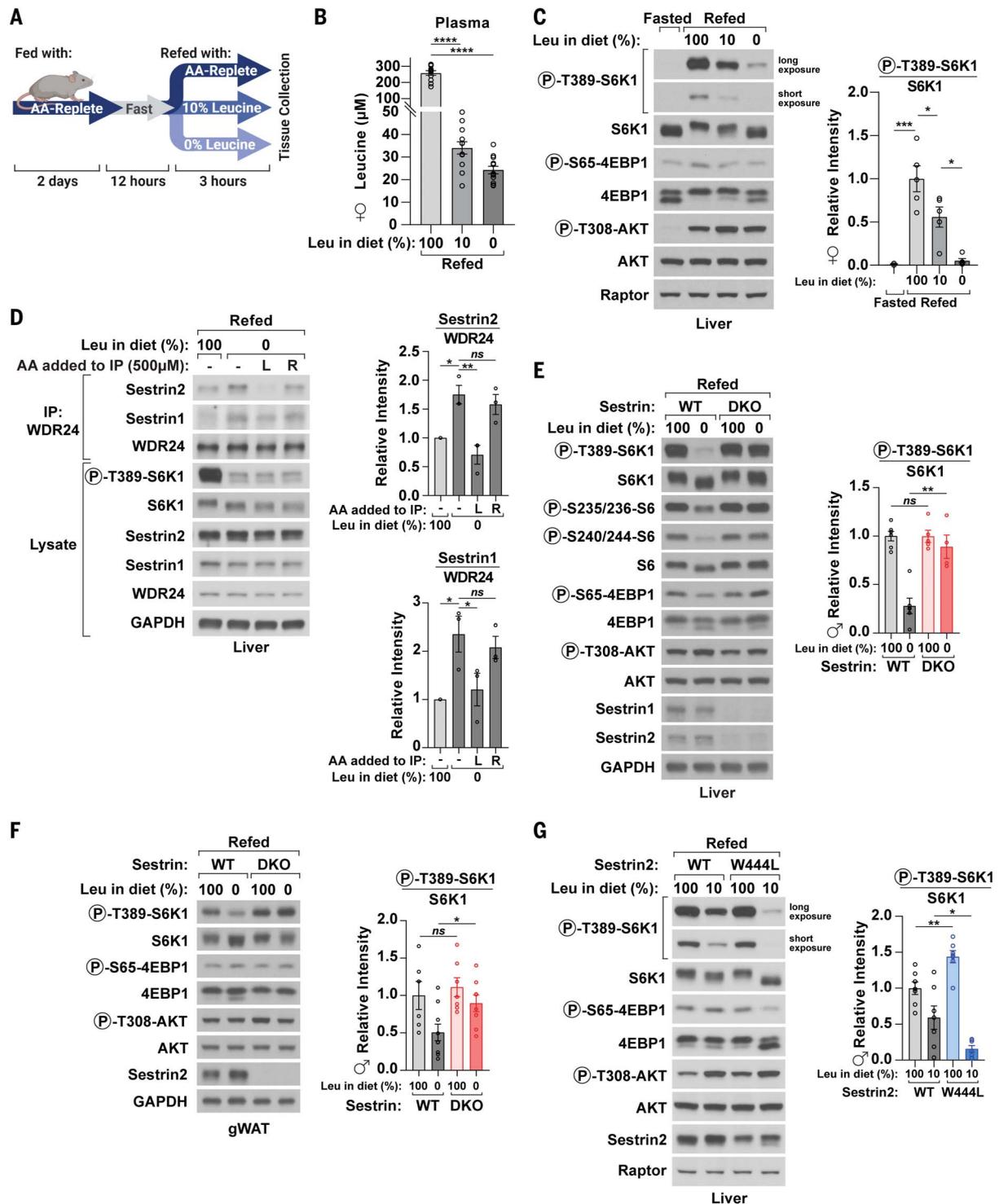
Fig. 1. The Sestrins control leucine sensing by mTORC1 in vivo.
(**A**) Schematic of the experimental setup for studying leucine sensing in vivo. Mice maintained on an amino acid (AA)–replete control diet for 2 days were fasted overnight for 12 hours then refed with food containing the indicated leucine contents, and tissues were collected 3 hours after the start of the feeding period. (**B**) Plasma leucine concentrations in wild-type female mice 3 hours after eating the indicated diets (n = 11 to 12 mice). (**C**) Phosphorylation state and amounts of indicated proteins in liver lysates from wild-type female mice refed with the indicated diets for 3 hours (n = 3 to 5 mice). (**D**) Dietary leucine regulates Sestrin-GATOR2 interactions. Endogenous WDR24 immunoprecipitates

(IPs) were prepared from liver lysates from wild-type male mice refed with the indicated diets for 3 hours. In lanes 2 to 4, IPs were prepared from equal volumes of the same liver lysate, and, where noted, indicated amino acids were added during washes. L, leucine; R, arginine; GAPDH, glyceraldehyde phosphate dehydrogenase. IPs and liver lysates were analyzed by immunoblotting for the phosphorylation states and amounts of the indicated proteins (n = 3 mice). (**E**) Male mice with indicated genotypes were refed with the indicated diets for 3 hours. Liver lysates were analyzed by immunoblotting for the phosphorylation state and amounts of the indicated proteins (n = 4 to 6 mice). (**F**) Gonadal WAT (gWAT) lysates from

male mice treated as in (E) were analyzed by immunoblotting for the phosphorylation states and amounts of the indicated proteins (*n* = 6 to 9 mice). (**G**) Female mice with the indicated liver genotypes were refed with diets with different leucine contents for 3 hours, and liver lysates were analyzed by immunoblotting for the phosphorylation state and amounts of the indicated proteins (*n* = 7 mice). Data are the mean ± SEM. *P* values were determined using two-tailed *t* tests [(B) and (E) to (G)], one-way analysis of variance (ANOVA) with Tukey test [(B) and (C)], or one-way ANOVA with Dunnett's test (D). *$P < 0.05$, **$P < 0.01$, ***$P < 0.001$, ****$P < 0.0001$. ns, not significant.

of Sestrin2 for leucine (*33*). To determine how this mutation affects the activation of mTORC1 by leucine in vivo, we generated knockin mice expressing Sestrin2 W444L from the endogenous *Sesn2* locus (*Sesn2^{W444L}* mice). Leucine, over a range of concentrations, activated mTORC1 to a lesser degree in primary hepatocytes from *Sesn2^{W444L}* than control (*Sesn2^{WT}*) mice (fig. S2F). Similarly, food containing 10% of the leucine content of normal chow activated mTORC1 to a lesser extent in the livers of *Sesn2^{W444L}* than *Sesn2^{WT}* mice (Fig. 1G). Thus, the affinity of Sestrin2 for leucine determines the sensitivity of mTORC1 to the leucine content of the diet. Taken together, our results establish that, as in cultured cells, Sestrin1 and Sestrin2 transmit leucine availability to the mTORC1 pathway in vivo.

Sestrin-mediated leucine sensing preserves WAT and muscle mass during dietary leucine deprivation

To examine the physiological importance of leucine sensing by mTORC1, we fed wild-type and DKO mice lacking Sestrin1 and Sestrin2 the leucine-free diet for 8 days (Fig. 2A). DKO mice, but not *Sesn1^{−/−}* mice or *Sesn2^{−/−}* mice, lost more body weight than wild-type controls (Fig. 2B and fig. S3) despite eating similar amounts of the leucine-free food (fig. S4). The greater reduction in body weight in DKO mice was a consequence of a severe loss of WAT, as evident in gross and microscopic examinations of several fat depots, as well as a reduction in skeletal muscle mass (Fig. 2, C to G). We saw these phenotypes in both sexes (fig. S5), although the WAT loss was more pronounced in female mice. Liver mass did not contribute to the difference in body weight, as it was unaffected by Sestrin loss (fig. S6). Although wild-type and DKO mice ate a similarly reduced amount of the leucine-free food in comparison with control food (fig. S4), this reduction in food intake does not account for the different responses of wild-type and DKO mice to leucine-free feeding (fig. S7, A to C). Furthermore, the reductions in body weight, WAT, and skeletal muscle occurred in leucine-deprived DKO mice regardless of whether they were fasted before feeding with the leucine-free diet (fig. S7, D to F). As mTORC1 activity and leucine deprivation can both affect insulin signaling and glucose homeostasis (*4*, *40*, *41*), we assessed glucose tolerance, insulin secretion, and hepatic insulin sensitivity but found no alterations in the DKO mice (fig. S8). On

the leucine-free diet, wild-type and DKO mice had similarly low levels of plasma leucine (Fig. 2H and fig. S9). However, whereas plasma levels of several other amino acids were either maintained or in some cases even increased in wild-type mice, levels of those same amino acids were reduced in DKO mice (Fig. 2H and fig. S9).

Treatment with rapamycin, an mTORC1 inhibitor, restored the total body weight and WAT mass of DKO mice to those of wild-type animals (fig. S10). Aberrant mTORC1 activity thus underlies the inappropriate response of DKO mice to leucine deprivation.

Notably, on diets lacking valine or methionine, DKO and wild-type mice lost equal amounts of total body weight, WAT, and skeletal muscle (Fig. 2, I to N). The lack of altered responses in DKO mice to these diets is consistent with the Sestrins being specific sensors of leucine at physiological amino acid concentrations (*32*).

Lastly, *Sesn2^{W444L}* mice, in which mTORC1 is inhibited more strongly upon leucine deprivation than in wild-type animals (Fig. 1G), lost less WAT mass than control *Sesn2^{WT}* mice over an extended period (16 days) of leucine deprivation (Fig. 2, O to Q), despite having similar intake of the leucine-free food (fig. S11A). Thus, the leucine-binding capacity of Sestrin2 modulates the physiological response to leucine deprivation. In contrast, leucine-deprived *Sesn2^{W444L}* and *Sesn2^{WT}* mice lost similar amounts of skeletal muscle (fig. S11, B to D), consistent with muscle not expressing detectable levels of Sestrin2 (fig. S11E) (*42*). We conclude that mice require the Sestrin-mediated regulation of mTORC1 to maintain homeostasis specifically in response to limited leucine availability.

Leucine sensing in the liver controls the response of WAT to dietary leucine deprivation through FGF21

Because adipocyte-specific hyperactivation of mTORC1 can lead to a reduction in WAT mass (*43*), we considered the possibility that mTORC1 deregulation in the adipocytes of the WAT itself (Fig. 1F and figs. S1E and S2D) might cause its loss in DKO mice on the leucine-free diet. Although mice lacking both Sestrin1 and Sestrin2 only in adipose tissue (AdiDKO mice) lack mTORC1 regulation in the WAT in response to leucine (fig. S12, A and B), they did not phenocopy DKO mice when fed the leucine-free diet (fig. S12, C to E), indicating

that Sestrin loss affects WAT mass through a tissue-nonautonomous mechanism.

Given that hepatic mTORC1 can regulate organismal physiology (*44–46*) and is sensitive to dietary leucine in a Sestrin-dependent manner (Fig. 1E and fig. S1A), we hypothesized a central role for the Sestrins in the liver in the response to leucine limitation. Indeed, in mice lacking both Sestrins in the liver (LiDKO mice), leucine deprivation caused a greater loss of body weight than in wild-type and *Sesn2^{−/−}* mice, albeit not as pronounced as in DKO mice (Fig. 3A). As DKO mice lose both WAT and muscle mass upon leucine deprivation (Fig. 2, C to G), we sought to determine what accounted for the reduction in body weight of LiDKO mice. On the leucine-free diet, LiDKO mice phenocopied the severe WAT loss of DKO mice (Fig. 3, B to D) but had muscle mass and plasma amino acid concentrations similar to those in wild-type animals (Fig. 3E and fig. S13). The WAT loss of DKO and LiDKO mice is unlikely to be the consequence of an unrecognized developmental defect, as the AAV-Cre–mediated acute deletion of Sestrin1 and Sestrin2 in the livers of adult mice conferred the same phenotype (fig. S14).

Together, our results indicate that hepatic Sestrin-mTORC1 plays a key role in the organismal response to leucine deprivation and suggest that liver-to-WAT communication controls the WAT loss observed in DKO mice. The two other phenotypes we documented in DKO mice—loss of muscle mass and deregulation of plasma amino acid concentrations upon leucine starvation—are independent of Sestrin function in the liver and are perhaps mediated by the Sestrins in muscle, given the importance of muscle for maintaining circulating amino acid concentrations (*47–50*). Thus, mice require leucine-sensitive Sestrin function in several tissues to maintain homeostasis upon removal of dietary leucine.

Among its many functions, the liver is a source of circulating factors, or hepatokines, that promote metabolic homeostasis. Among these, we focused on fibroblast growth factor 21 (FGF21), as it is implicated in the response to amino acid starvation and WAT remodeling (*51–53*). Upon leucine deprivation, plasma FGF21 concentrations were higher in DKO than wild-type mice (Fig. 4A) but similar when mice were fed an amino acid–replete diet (Fig. 4A) or fasted (fig. S15A). In DKO mice, FGF21 mediates the exacerbated loss of body weight and WAT during leucine deprivation, as its
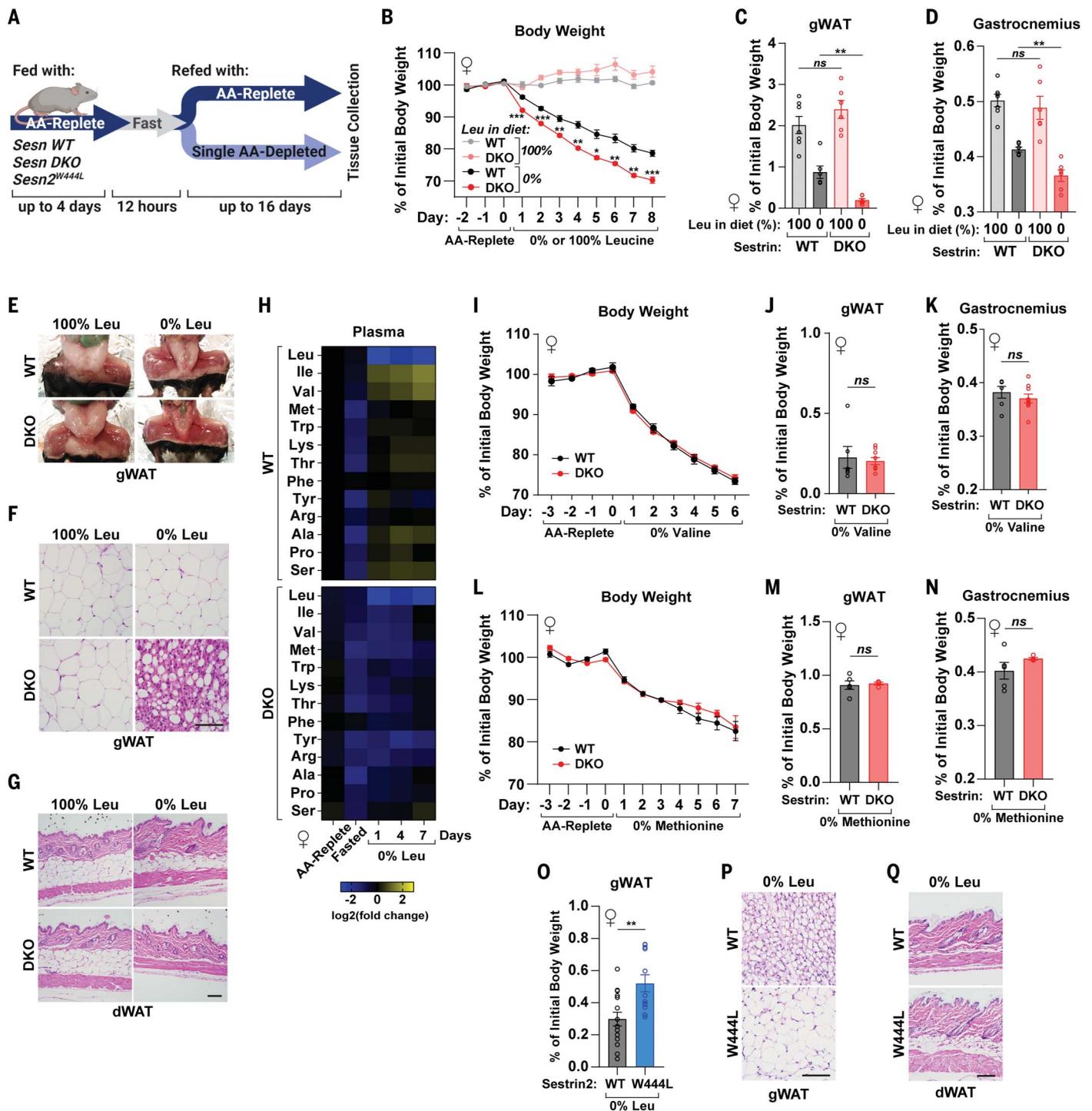
Fig. 2. Mice require Sestrin1 and Sestrin2 to adapt to limitations in dietary leucine. (**A**) Experimental setup for studying the long-term impacts of depriving mice of individual amino acids. Mice of the indicated genotypes were maintained on an amino acid–replete control diet for up to 4 days, fasted overnight for 12 hours, and then refed with the control diet or food lacking an essential amino acid for up to 16 days. (**B**) Body weights of female mice of the indicated genotypes during feeding with the indicated diets (n = 6 to 7 mice). The daily body weight measurements of each mouse during initial maintenance on an amino acid–replete control diet were averaged; the percent change from this average is depicted. (**C** and **D**) Gonadal WAT (C) and gastrocnemius muscle weights (D) in female mice of the indicated genotypes after 8 days on the indicated diets (n = 6 to 7 mice). Tissue weights for each

mouse are presented as the percent of the average body weight while on an amino acid–replete control diet. (**E**) Representative images of gonadal WAT from female mice of the indicated genotypes after 8 days on the indicated diets (n = 6 to 7 mice). (**F** and **G**) Hematoxylin and eosin (H&E) stain of gonadal WAT (F) and dermal WAT (dWAT) (G) pad sections from female mice of the indicated genotypes after 8 days on the indicated diets. Images are representative of 6 to 7 mice. Scale bars, 50 μm. (**H**) Relative plasma abundances of amino acids from serial blood sampling of female mice of the indicated genotypes, which were kept on an amino acid–replete diet, fasted for 12 hours overnight, and then refed with a leucine-free diet for up to 7 days. Data are presented as log$_2$ fold change of mean values relative to those in wild-type mice on the control diet (n = 3 to 5 mice). Amino acids with significant changes

($P < 0.05$) during leucine-free feeding as compared with the amino acid–replete condition are shown. See fig. S9 for all amino acids and statistical analyses. (**I**) Body weights of female mice of the indicated genotypes on a valine-free diet (n = 6 to 9 mice). The daily body weight measurements of each mouse during initial maintenance on an amino acid–replete control diet were averaged; the percent change from this average is depicted. (**J** and **K**) Gonadal WAT (J) and gastrocnemius muscle weight (K) of female mice of the indicated genotypes after 8 days of feeding on a valine-free diet (n = 6 to 9 mice). Tissue weight for each mouse is presented as percent of the average body weight while on the amino acid–replete control diet. (**L** to **N**) Same analyses as in (I) to (K), respectively,

except mice were fed a methionine-free diet (n = 4 to 5 mice). (**O**) Gonadal WAT weight of female mice of the indicated genotypes after 16 days of feeding with a leucine-free diet (n = 12 to 15 mice). Tissue weight for each mouse is presented as percent of the average body weight while initially kept on the amino acid–replete control diet for 4 days. (**P** and **Q**) H&E stain of gonadal (P) and dermal (Q) WAT pad sections from female mice of the indicated genotypes after 16 days of feeding with a leucine-free diet. Images are representative of 6 to 8 mice. Scale bars, 50 µm. Data are the mean ± SEM. P values were determined using repeated measures two-way ANOVA with Sidak test [(B), (I), and (L)] or two-tailed t tests [(C), (D), (J), (K), and (M) to (O)]. *$P < 0.05$, **$P < 0.01$, ***$P < 0.001$.
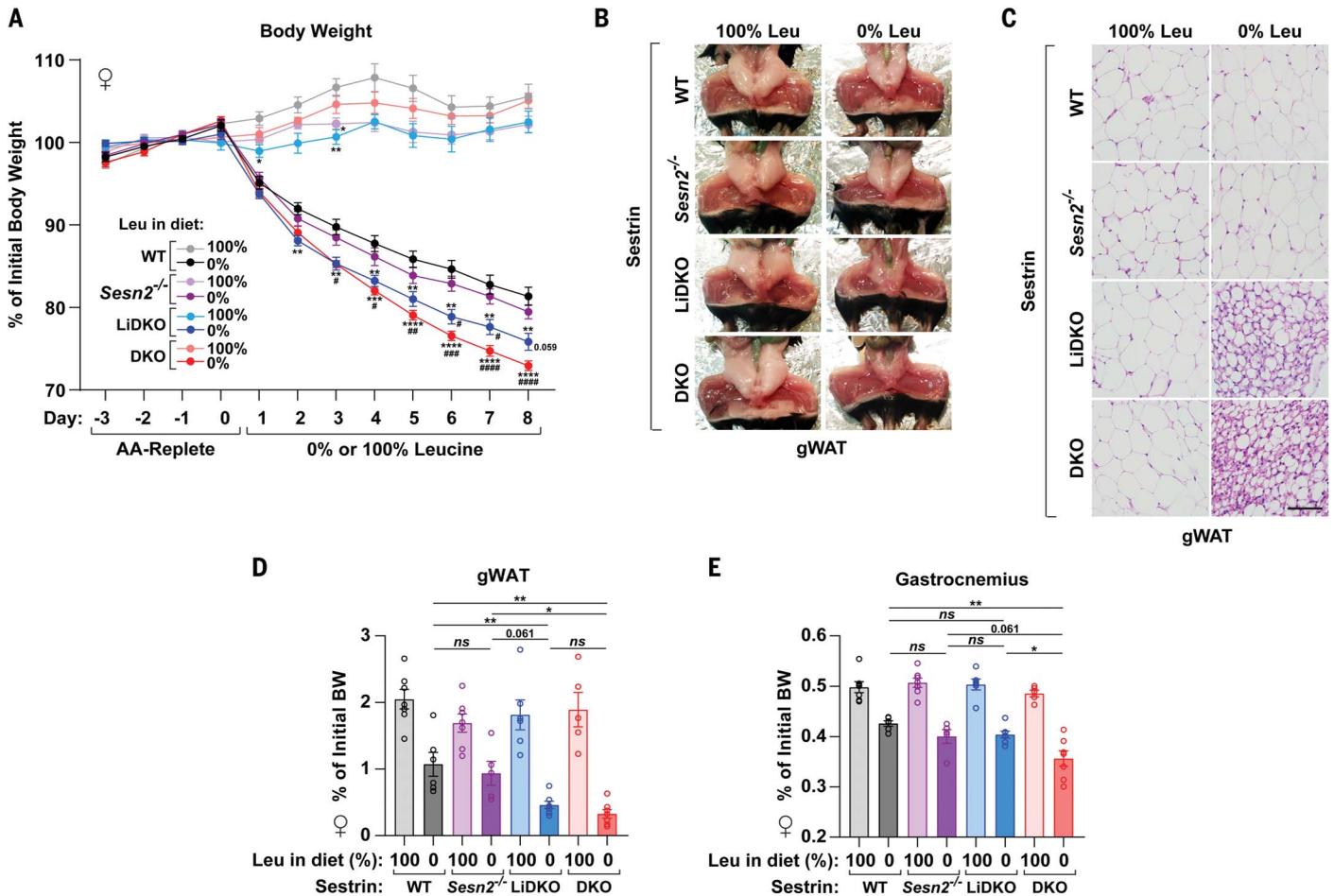

Fig. 3. Liver Sestrins control WAT remodeling upon deprivation of dietary leucine. (**A**) Body weights of female mice of the indicated genotypes fed the indicated diets (n = 5 to 12 mice). The daily body weight measurements of each mouse during initial maintenance on an amino acid–replete control diet were averaged; the percent change from this average is depicted. Statistical comparisons to the wild-type group (*) and the $Sesn2^{-/-}$ group (#) are shown. (**B**) Images of gonadal WAT in female mice of the indicated genotypes after 8 days on the indicated diets. Images are representative of 3 to 4 mice. (**C**) H&E analyses of gonadal WAT sections from female mice of the indicated genotypes after 8 days on the indicated diets. Images are representative of 3 to 4 mice. Scale bar, 50 µm. (**D** and **E**) Gonadal WAT (D) and gastrocnemius muscle (E) weights of female mice with the indicated genotypes after 8 days on a leucine-free diet (n = 5 to 7 mice). Tissue weights of each mouse are presented as percent of the average body weight (BW) on the amino acid–replete control diet. Data are the mean ± SEM. P values were determined using repeated measures two-way ANOVA with Tukey test (A) or one-way ANOVA with Tukey test [(D) and (E)]. *$P < 0.05$, **$P < 0.01$.

deletion prevented these effects (Fig. 4, B to E, and fig. S15, B to D). When deprived of leucine, DKO and LiDKO mice had similar increases in plasma FGF21 (Fig. 4A), pinpointing the liver as the likely source of the FGF21. Correspondingly, leucine deprivation increased the amount of *Fgf21* mRNA in the liver of DKO mice (fig. S15E), resulting in a boost in hepatic FGF21 protein amounts that strongly correlated with those in the plasma (fig. S15F). Consistent with estrogen signaling potentiating hepatic FGF21 production (*54*), FGF21
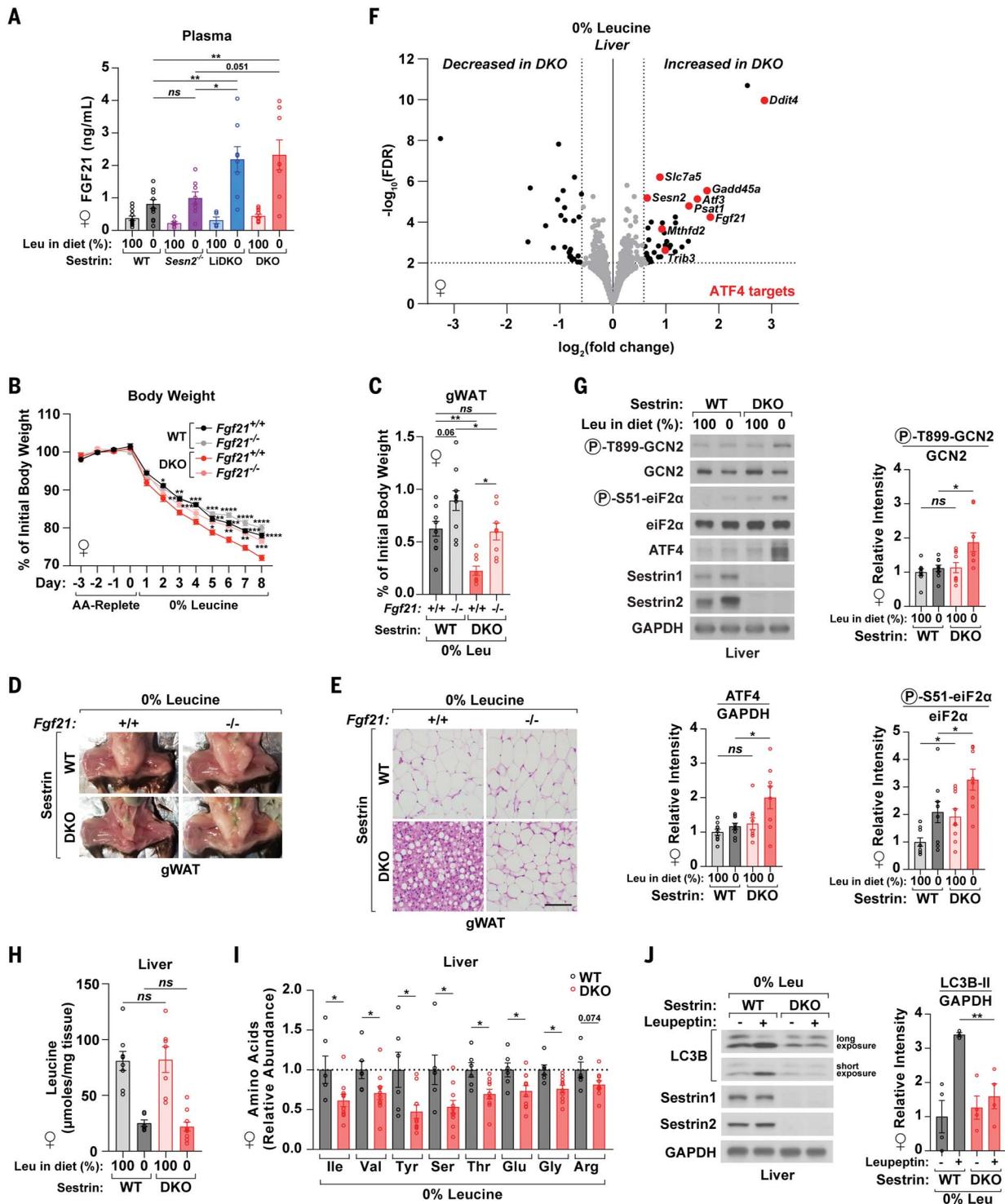
Fig. 4. During dietary leucine deprivation, Sestrins in the liver control WAT maintenance through FGF21 production. (**A**) Plasma FGF21 concentrations in female mice of the indicated genotypes 24 hours after feeding with the indicated diets (*n* = 5 to 12 mice). (**B**) Body weights of female mice of the indicated genotypes during feeding with a leucine-free diet (*n* = 5 to 10 mice). The daily body weight measurements of each mouse during initial maintenance on an amino acid–replete control diet were averaged; the percent change from this average is depicted. Statistical comparisons to the DKO group are shown. (**C**) Gonadal WAT weight of female mice with the indicated genotypes after 8 days on a leucine-free diet (*n* = 5 to 10 mice). Tissue weights of each mouse

are presented as percent of the average body weight on the amino acid–replete control diet. (**D**) Images of gonadal WAT in female mice of the indicated genotypes after 8 days on a leucine-free diet. Images are representative of 5 to 10 mice. (**E**) H&E analyses of gonadal WAT sections from female mice of the indicated genotypes after 8 days on a leucine-free diet. Images are representative of 5 to 10 mice. Scale bar, 50 μm. (**F**) Volcano plot of genes differentially expressed in WT and DKO livers after 24 hours of leucine-free feeding (*n* = 7 to 18 mice). Transcripts that are differentially expressed ≥1.5-fold with a false discovery rate (FDR) of <0.01 are depicted in black. Among these, ATF4 target genes are depicted in red. For better visualization, *Sesn1* [log$_2$(fold change) = −1.60;

−log$_{10}$(FDR) = 79.87] was excluded from the plot. *Sesn2* reads in DKO mice are derived from nonfunctional transcripts generated by the *Sesn2* null allele. See fig. S16 for additional analysis. (**G**) Female mice of the indicated genotypes were fed with the indicated diets for 24 hours, and liver lysates were analyzed by immunoblotting for the phosphorylation state and amounts of the indicated proteins (*n* = 8 to 9 mice). (**H**) Quantification of leucine in the livers of female mice of the indicated genotypes after 24 hours of feeding with the indicated diets (*n* = 6 to 10 mice). Molar quantities are normalized to tissue weights. (**I**) Relative abundances of amino acids in the livers of female mice of the indicated genotypes after 24 hours of feeding with a leucine-free diet. Abundances are normalized to tissue weights

and shown relative to the average abundances in wild-type livers (*n* = 6 to 10 mice). Data were acquired from the same samples as in (H). Amino acids with significant changes (*P* < 0.05) are shown. See fig. S20A for data for all amino acids and experimental groups. (**J**) Female mice of the indicated genotypes were treated with leupeptin or vehicle for 4 hours after 24 hours of feeding with a leucine-free diet. Liver lysates were analyzed by immunoblotting for amounts of the indicated proteins (*n* = 3 to 4 mice). Data are the mean ± SEM. *P* values were determined using one-way ANOVA with Tukey test [(A) and (C)], repeated measures two-way ANOVA with Tukey test (B), or two-tailed *t* test [(G) to (J)]. *P < 0.05, **P < 0.01, ***P < 0.001, ****P < 0.0001.

concentrations increased less in male than female DKO mice deprived of leucine (fig. S15G), perhaps accounting for the more modest loss of WAT observed in males (fig. S5C).

Fgf21 expression in the liver is transcriptionally regulated by several mechanisms, including the transcription factor ATF4 (*55–57*). Transcriptome analysis revealed that during leucine deprivation, DKO mice strongly induced ATF4 activity in the liver, as they had increased expression of many ATF4 target genes compared with leucine-deprived wild-type controls at short (24 hours) and long (8 days) timepoints after the start of the leucine-free diet (Fig. 4F and fig. S16). ATF4 is induced by eukaryotic translation initiation factor 2 subunit alpha (eIF2α) phosphorylation during the integrated stress response (ISR) (*58*). Consistent with activation of the ISR in the livers of DKO mice, leucine starvation led to an increase in eIF2α phosphorylation and ATF4 protein (Fig. 4G). Independently of eIF2α, mTORC1 itself can also promote *Atf4* mRNA translation (*59*, *60*) and so may contribute to the observed increase in ATF4 protein. Oxidative stress can also induce ATF4 (*61*, *62*), but we observed no differences in redox state between wild-type and DKO livers during leucine deprivation, as indicated by the ratios of GSH:GSSG, NADH:NAD+, and AMP:ATP (fig. S17, A to C).

Several stress-activated kinases can phosphorylate eIF2α, including PERK, which responds to endoplasmic reticulum (ER) stress, and GCN2, which is activated by the uncharged tRNAs that accumulate when amino acids are limiting for tRNA aminoacylation (*63*). Leucine starvation did not increase PERK autophosphorylation, a marker of its activity, as compared with treatment with tunicamycin, a canonical activator of ER stress (fig. S17D). In contrast, leucine deprivation strongly and rapidly boosted GCN2 activity (indicated by its autophosphorylation) and ATF4 target gene expression in the liver during the initial 3 to 6 hours of refeeding with the leucine-free diet (figs. S18 and S19). Notably, while wild-type mice largely showed suppression of this initial ISR induction with-

in 24 hours of leucine starvation, DKO mice retained elevated GCN2 activity (Fig. 4G), suggesting that the Sestrins are required for the liver to maintain amino acid homeostasis during leucine deprivation. Indeed, while leucine starvation reduced leucine to equally low levels in the livers of both wild-type and DKO mice (Fig. 4H and fig. S20A), wild-type mice largely maintained or even increased the levels of other proteogenic amino acids in the liver, but DKO mice did not and had lower hepatic levels of several amino acids (Fig. 4I and fig. S20A).

A major source of amino acids in the liver is the degradation of proteins by autophagy (*64*, *65*), a process suppressed by mTORC1 through inhibitory phosphorylation of the kinase ULK1 (*4*, *21–23*). Notably, many of the amino acids reduced in the livers of DKO mice, particularly isoleucine, valine, threonine, tyrosine, and serine, are also affected in the livers of mice with hepatic autophagy disruption (*65*). We therefore examined autophagic flux by measuring LC3B lipidation after treating mice with the lysosomal protease inhibitor leupeptin (*66*, *67*). Compared with a control diet, leucine deprivation increased autophagic flux in wild-type livers (fig. S20B). In contrast, in DKO mice, leucine deprivation did not relieve the inhibitory phosphorylation of ULK1 by mTORC1 (fig. S20C) or induce autophagic flux (Fig. 4J), providing a likely explanation for their activation of GCN2 and expression of ATF4 and FGF21.

Protein synthesis can also affect levels of amino acids through their consumption and is regulated by both mTORC1 and GCN2 (*68*). However, we found no significant impact of Sestrin expression on protein synthesis in the liver, as assessed by polysome profiling and puromycin incorporation into protein (fig. S21).

In DKO mice on the leucine-free diet, inhibition of mTORC1 with rapamycin attenuated the aberrant phosphorylation of mTORC1 substrates, drop in hepatic amino acids, ATF4 target gene expression, and plasma FGF21 concentrations (fig. S22). Together, these results confirm that, as with WAT mass (fig. S10,

B to D), the Sestrins affect leucine-sensitive physiology through mTORC1.

Leucine sensing is spatially compartmentalized in the liver and drives a zonated response to dietary leucine deprivation

Within the liver, hepatocytes are organized into a large number of hexagonally shaped lobules. Nutrient-rich blood coming from the gastrointestinal tract enters the periphery of each lobule through branches of the portal vein and percolates through sinusoids between the hepatocytes before exiting at the central vein. Hepatocytes in different zones of the lobule can have distinct metabolic functions and transcriptional programs (*69*, *70*), so we reasoned that there might be a spatial organization to Sestrin1 and Sestrin2 expression within the liver lobule. Indeed, using single-molecule fluorescence in situ hybridization, we observed zonated expression of the *Sesn1* and *Sesn2* mRNAs, with many transcripts in periportal and midlobular hepatocytes and fewer in the pericentral hepatocytes marked by *Glul* expression (Fig. 5A and fig. S23, A to C). This finding suggested that there also might be zonal differences in the leucine sensitivity of mTORC1 signaling, which we monitored using an immunofluorescence assay for phosphorylated S6, a marker of mTORC1 activity. Notably, mTORC1 activity was not uniform across the liver lobule in wild-type mice fed a leucine-free diet. It was inhibited in the periportal and midlobular hepatocytes that express Sestrin but active in the pericentral ones that do not. In contrast, in DKO mice starved of leucine, mTORC1 activity was uniform across the lobule and indistinguishable from that in mice fed amino acid–replete food (Fig. 5B and fig. S23D).

To understand the impact of zonated mTORC1 activity, we determined the spatial pattern of *Fgf21* expression in wild-type and DKO mice. *Fgf21* was minimally expressed in the livers of mice fed a control diet but was induced upon leucine deprivation in the periportal and midlobular hepatocytes that express Sestrin. This induction was amplified by Sestrin loss (Fig. 5C and fig. S23E), consistent
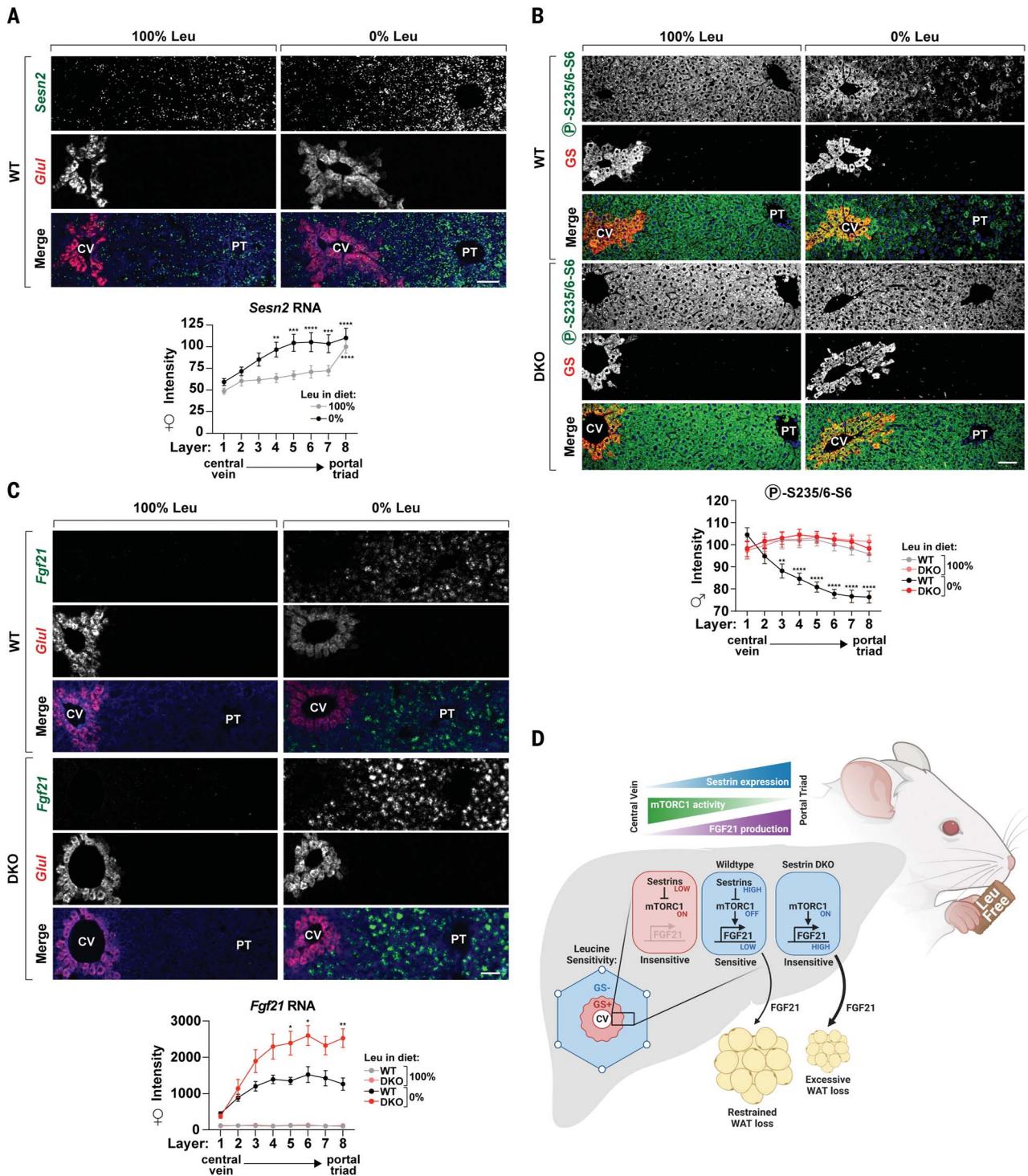
Fig. 5. Zonated Sestrin expression establishes leucine-sensitive and leucine-insensitive compartments in the liver. (**A**) Representative images and quantification of *Sesn2* mRNA in the livers of wild-type female mice 24 hours after feeding with the indicated diets (16 to 18 lobules from three mice per diet). *Glul* encoding glutamine synthetase marks pericentral hepatocytes. Shown are statistical comparisons to layer 1 for each diet. (**B**) Representative images and quantification of S6 phosphorylation as detected in immunofluorescence assays in liver sections from female mice of the indicated liver genotypes 3 hours after refeeding with the indicated diets (12 to 24 lobules from four to seven mice per genotype per diet). GS indicates glutamine synthetase and marks pericentral hepatocytes. Statistical comparisons between genotypes on the leucine-free diet are shown. (**C**) Representative images and quantification of *Fgf21* mRNA in liver sections of female mice of the indicated genotypes after 24 hours of feeding with the indicated diets (7 to 16 lobules from three mice per genotype per diet). *Glul* encoding glutamine synthetase marks pericentral hepatocytes. Statistical comparisons between genotypes on the leucine-free diet are shown. (**D**) Model of zonated leucine sensing by Sestrin-mTORC1 in the liver and its role in the physiological response to dietary leucine deprivation. CV, central vein; PT, portal triad. Scale bars, 50 μm. Data are the mean ± SEM. *P* values were determined using two-way ANOVA with Dunnett's test (A) or two-way ANOVA with Sidak test [(B) and (C)]. *$P < 0.05$, **$P < 0.01$, ***$P < 0.001$, ****$P < 0.0001$.

with the increase in ATF4 detected by immunoblotting (Fig. 4G). Furthermore, *Sesn2*, which is itself an ATF4 target (*71*), was also induced by leucine deprivation in wild-type mice (Fig. 4G) in the same zones as *Fgf21* (Fig. 5, A and C). The pericentral hepatocytes did not activate the ISR during leucine deprivation, as indicated by their lack of *Fgf21* induction, despite maintaining high mTORC1 activity. This suggests that they are intrinsically resistant to the negative effects of leucine deprivation, perhaps accounting for why they are wired to have low Sestrin expression. The lack of ISR activation in these cells may itself contribute to their low expression of *Sesn2*, as it is an ATF4 target gene. The resistance of the pericentral hepatocytes may stem from known features of these cells, including their constitutively high levels of autophagy (*72*, *73*), expression of ER chaperones (*74*), and synthesis of intracellular glutamine whose efflux can drive leucine uptake (*75*). We conclude that in the liver, the Sestrin-imposed and zone-specific regulation by leucine of mTORC1 signaling is necessary to attenuate the stress of dietary leucine deprivation (Fig. 5D).

Discussion

The nature of the leucine sensing pathway upstream of mTORC1 has been controversial, and many diverse sensors and mechanisms have been proposed to play a role (*24–31*), largely on the basis of work in cultured cells. We find that Sestrin1 and Sestrin2 control mTORC1 activity in response to leucine in vivo and that this modulation is necessary for mice to adapt to limitations in dietary leucine. These data, along with previous biochemical and structural work (*32*, *33*), are consistent with Sestrin1 and Sestrin2 being leucine sensors for the mTORC1 pathway. It has been proposed that the Sestrins can function through AMPK (*31*), but we found that AMPK is not required for dietary leucine to regulate mTORC1 in our model system. This does not preclude the possibility, however, that Sestrin loss may secondarily affect AMPK, because mTORC1 activity is known to drive energetic stress (*76*).

Further, our results suggest a temporal relationship between the activities of mTORC1 and GCN2 in the response to dietary leucine deficiency, in which Sestrin-mediated mTORC1 inhibition is necessary to maintain amino acid homeostasis and attenuate GCN2 activity during prolonged, but not acute, leucine deprivation. As GCN2 also modulates mTORC1 activity through ATF4-mediated *Sesn2* expression (*71*), our data reflect a homeostatic mechanism of reciprocal cross-talk between these amino acid–sensitive kinases.

We also reveal a previously unappreciated complexity to nutrient sensing by mTORC1 in vivo. In the liver lobule, only hepatocytes in certain zones appreciably express the Sestrins,

and only in these zones is mTORC1 signaling sensitive to dietary leucine. In considering why this might be the case, it is worth recalling that mTORC1 controls a large number of metabolic pathways and is also regulated by a diverse set of nutrients (*4*, *21–23*). Such an arrangement sets up a conundrum: How can mTORC1 regulate a metabolic pathway in response to the concentrations of a specific nutrient—such as one consumed by the pathway—but not to others to which sensitivity would be unfavorable?

We hypothesize that, at least in the liver, the zonated expression of nutrient sensors is part of the answer, along with the well-appreciated zonation of many metabolic processes. Although at the whole-liver level we were unable to detect changes in protein synthesis, it is noteworthy that the periportal hepatocytes that express the Sestrins also have been reported to play a predominant role in liver protein synthesis (*77*, *78*), a process that can be regulated by mTORC1 and consumes leucine. Conversely, the pericentral hepatocytes that have low Sestrin expression are the main site of ketogenesis, a process that mTORC1 can inhibit (*47*) but for which leucine sensitivity would be inappropriate given that an abundant supply of dietary glucose, regardless of leucine availability, renders ketones redundant as a fuel source. The combinatorial impact of the zonated expression of the nutrient sensors that signal to mTORC1 and of the metabolic processes controlled by it may underlie how one pathway can appropriately regulate such a variety of metabolic processes in response to diverse nutritional states.

REFERENCES AND NOTES

1. M. Wallace et al., Nat. Chem. Biol. **14**, 1021–1031 (2018).
2. S. B. Crown, N. Marze, M. R. Antoniewicz, PLOS ONE **10**, e0145850 (2015).
3. J. Rosenthal, A. Angel, J. Farkas, Am. J. Physiol. **226**, 411–418 (1974).
4. R. A. Saxton, D. M. Sabatini, Cell **168**, 960–976 (2017).
5. J. C. Anthony et al., J. Nutr. **130**, 2413–2419 (2000).
6. Y. Duan et al., Front. Biosci. (Landmark Ed.) **20**, 796–813 (2015).
7. Y. Yin et al., Amino Acids **39**, 1477–1486 (2010).
8. F. Li, Y. Yin, B. Tan, X. Kong, G. Wu, Amino Acids **41**, 1185–1193 (2011).
9. W. T. Moore et al., Curr. Diab. Rep. **15**, 76 (2015).
10. C. A. de Oliveira, M. Q. Latorraca, M. A. de Mello, E. M. Carneiro, Amino Acids **40**, 1027–1034 (2011).
11. J. Yang, Y. Chi, B. R. Burkhardt, Y. Guan, B. A. Wolf, Nutr. Rev. **68**, 270–279 (2010).
12. E. A. Ananieva, J. D. Powell, S. M. Hutson, Adv. Nutr. **7**, 798S–805S (2016).
13. W. Ren et al., Cell Death Dis. **8**, e2655 (2017).
14. M. Torigoe et al., Mod. Rheumatol. **29**, 885–891 (2019).
15. N. E. Richardson et al., Nat. Aging **1**, 73–86 (2021).
16. G. D'Antona et al., Cell Metab. **12**, 362–372 (2010).
17. S. M. Solon-Biet et al., Nat. Metab. **1**, 532–545 (2019).
18. C. B. Newgard et al., Cell Metab. **9**, 311–326 (2009).
19. C. J. Lynch, S. H. Adams, Nat. Rev. Endocrinol. **10**, 723–736 (2014).
20. L. Fontana et al., Cell Rep. **16**, 520–530 (2016).
21. G. Y. Liu, D. M. Sabatini, Nat. Rev. Mol. Cell Biol. **21**, 183–203 (2020).
22. K. J. Condon, D. M. Sabatini, J. Cell Sci. **132**, jcs222570 (2019).
23. A. J. Valvezan, B. D. Manning, Nat. Metab. **1**, 321–333 (2019).
24. J. M. Han et al., Cell **149**, 410–424 (2012).
25. J. H. Kim et al., Nat. Commun. **8**, 732 (2017).
26. X. D. He et al., Cell Metab. **27**, 151–166.e6 (2018).
27. R. V. Durán et al., Mol. Cell **47**, 349–358 (2012).
28. J. F. Linares et al., Mol. Cell **51**, 283–296 (2013).
29. R. E. Lawrence et al., Nat. Cell Biol. **20**, 1052–1063 (2018).
30. S. M. Son et al., Cell Metab. **29**, 192–201.e7 (2019).
31. A. V. Budanov, M. Karin, Cell **134**, 451–460 (2008).
32. R. L. Wolfson et al., Science **351**, 43–48 (2016).
33. R. A. Saxton et al., Science **351**, 53–58 (2016).
34. Z. Fang et al., Cell. Mol. Gastroenterol. Hepatol. **12**, 921–942 (2021).
35. B. A. Yang et al., Stem Cell Reports **16**, 2078–2088 (2021).
36. J. H. Lee et al., Cell Metab. **16**, 311–321 (2012).
37. J. Segalés et al., Nat. Commun. **11**, 189 (2020).
38. M. Kim et al., Nat. Commun. **11**, 190 (2020).
39. J. Lu et al., Nat. Aging **1**, 60–72 (2021).
40. F. Xiao et al., Diabetes **60**, 746–756 (2011).
41. S. Wei et al., Heliyon **4**, e00830 (2018).
42. D. Xu et al., Am. J. Physiol. Endocrinol. Metab. **316**, E817–E828 (2019).
43. J. Magdalon et al., Biochim. Biophys. Acta **1861**, 430–438 (2016).
44. S. Sengupta, T. R. Peterson, M. Laplante, S. Oh, D. M. Sabatini, Nature **468**, 1100–1104 (2010).
45. Y. Koketsu et al., Am. J. Physiol. Endocrinol. Metab. **294**, E719–E725 (2008).
46. M. Cornu et al., Proc. Natl. Acad. Sci. U.S.A. **111**, 11592–11599 (2014).
47. T. Pozefsky, R. G. Tancredi, R. T. Moxley, J. Dupre, J. D. Tobin, J. Clin. Invest. **57**, 444–449 (1976).
48. M. H. Vendelbo et al., PLOS ONE **9**, e102031 (2014).
49. G. F. Cahill Jr., N. Engl. J. Med. **282**, 668–675 (1970).
50. R. R. Wolfe, Am. J. Clin. Nutr. **84**, 475–482 (2006).
51. A. L. De Sousa-Coelho, P. F. Marrero, D. Haro, Biochem. J. **443**, 165–171 (2012).
52. A. L. De Sousa-Coelho et al., J. Lipid Res. **54**, 1786–1797 (2013).
53. T. Laeger et al., J. Clin. Invest. **124**, 3913–3922 (2014).
54. C. Allard et al., Mol. Metab. **22**, 62–70 (2019).
55. T. Lundåsen et al., Biochem. Biophys. Res. Commun. **360**, 437–440 (2007).
56. K. H. Kim et al., Nat. Med. **19**, 83–92 (2013).
57. R. Maruyama, M. Shimizu, J. Li, J. Inoue, R. Sato, Biosci. Biotechnol. Biochem. **80**, 929–934 (2016).
58. H. P. Harding et al., Mol. Cell **6**, 1099–1108 (2000).
59. M. E. Torrence et al., eLife **10**, e63326 (2021).
60. I. Ben-Sahra, G. Hoxhaj, S. J. H. Ricoult, J. M. Asara, B. D. Manning, Science **351**, 728–733 (2016).
61. P. S. Lange et al., J. Exp. Med. **205**, 1227–1242 (2008).
62. N. Miyamoto et al., Invest. Ophthalmol. Vis. Sci. **52**, 1226–1234 (2011).
63. R. C. Wek, H. Y. Jiang, T. G. Anthony, Biochem. Soc. Trans. **34**, 7–11 (2006).
64. J. Madrigal-Matute, A. M. Cuervo, Gastroenterology **150**, 328–339 (2016).
65. J. Ezaki et al., Autophagy **7**, 727–736 (2011).
66. M. Moulis, C. Vindis, Cells **6**, 14 (2017).
67. J. Haspel et al., Autophagy **7**, 629–642 (2011).
68. T. G. Anthony et al., J. Biol. Chem. **279**, 36553–36561 (2004).
69. K. B. Halpern et al., Nature **542**, 352–356 (2017).
70. K. Jungermann, N. Katz, Physiol. Rev. **69**, 708–764 (1989).
71. J. Ye et al., Genes Dev. **29**, 2331–2336 (2015).
72. R. Gebhardt, A. Hovhannisyan, Dev. Dyn. **239**, 45–55 (2010).
73. R. Gebhardt, P. J. Coffer, Cell Commun. Signal. **11**, 21 (2013).
74. C. Droin et al., Nat. Metab. **3**, 43–58 (2021).
75. P. Nicklin et al., Cell **136**, 521–534 (2009).
76. V. Aguilar et al., Cell Metab. **5**, 476–487 (2007).
77. R. Gebhardt, M. Matz-Soja, World J. Gastroenterol. **20**, 8491–8504 (2014).
78. Y. Uchiyama, A. Asari, Cell Tissue Res. **236**, 305–315 (1984).

SUPPLEMENTARY MATERIALS

science.org/doi/10.1126/science.abi9547
Materials and Methods
Figs. S1 to S23
Tables S1 and S2
References (79–83)
MDAR Reproducibility Checklist

View/request a protocol for this paper from *Bio-protocol*.

Science

Zonated leucine sensing by Sestrin-mTORC1 in the liver controls the response to dietary leucine

Andrew L. CangelosiAnna M. PuszynskaJustin M. RobertsAndrea ArmaniThao P. NguyenJessica B. SpinelliTenzin KunchokBrianna WangSze Ham ChanCaroline A. LewisWilliam C. CombGeorge W. BellAharon HelmanDavid M. Sabatini

Leucine sensing in the zone

Leucine is an essential amino acid that plays an important role in a variety of metabolic processes, including both physiological ones such as insulin secretion and pathological ones involved in the metabolic syndrome. mTORC1 is a key protein that is also involved in many aspects of metabolism and senses leucine through proteins called sestrins. Some aspects of this signaling pathway were previously observed in cultured cells, but now Cangelosi *et al.* have identified what happens in vivo in a mammal. The authors clarified the signaling steps involved in mTORC1 sensing of leucine through sestrins in mice and determined that the regulation of this pathway varies between different zones within the liver based on proximity to blood vessels. —YN

View the article online
https://www.science.org/doi/10.1126/science.abi9547
Permissions
https://www.science.org/help/reprints-and-permissions

Use of this article is subject to the Terms of service